Physics of the Dark Universe 12 (2016) 24–36

Contents lists available at ScienceDirect

Physics of the Dark Universe

journal homepage: www.elsevier.com/locate/dark

Continuum-mediated dark matter–baryon scattering

Andrey Katz [a,b,*], Matthew Reece [c], Aqil Sajjad [c]

[a] Theory Division, CERN, CH-1211 Geneva 23, Switzerland

[b] Université de Genève, Department of Theoretical Physics and Center for Astroparticle Physics (CAP), 24 quai E. Ansermet, CH-1211, Geneva 4, Switzerland

[c] Department of Physics, Harvard University, Cambridge, MA 02138, USA

ARTICLE INFO

Article history:
Received 25 September 2015
Received in revised form
17 January 2016
Accepted 17 January 2016

Keywords:
Dark matter direct detection
Dark matter models
Light dark matter mediators

ABSTRACT

Many models of dark matter scattering with baryons may be treated either as a simple contact interaction or as the exchange of a light mediator particle. We study an alternative, in which a continuum of light mediator states may be exchanged. This could arise, for instance, from coupling to a sector which is approximately conformal at the relevant momentum transfer scale. In the non-relativistic effective theory of dark matter–baryon scattering, which is useful for parametrizing direct detection signals, the effect of such continuum mediators is to multiply the amplitude by a function of the momentum transfer q, which in the simplest case is just a power law. We develop the basic framework and study two examples: the case where the mediator is a scalar operator coupling to the Higgs portal (which turns out to be highly constrained) and the case of an antisymmetric tensor operator $\mathcal{O}_{\mu\nu}$ that mixes with the hypercharge field strength and couples to dark matter tensor currents, which has an interesting viable parameter space. We describe the effect of such mediators on the cross sections and recoil energy spectra that could be observed in direct detection.

1. Introduction

Most of the matter in our universe, by mass, is dark matter, but beyond the fact that it interacts gravitationally, the nature of dark matter remains elusive. As experiments dig further into the parameter space of classic theories of dark matter and continue to find null results, it is important that we think as broadly as possible about what dark matter might be and how we might detect it. In this paper, we will suggest a novel form of interaction between dark matter and baryons and explore the extent to which it modifies the signals experiments searching for dark matter might observe.

In recent years, a much wider variety of possible dark matter models and phenomenology has begun to be explored. Non-relativistic effective theories have systematized the exploration of possible operators characterizing dark matter–baryon scattering in direct detection experiments [1–13], drawing on older work outside the dark matter context [14]. The basic operator approach can be modified in various ways, for instance through considering dark matter particles inelastically scattering to or from excited states [15–17], dark matter particles with form factors [18,19], dark matter that scatters through $2 \rightarrow 3$ processes [20,21], scattering of dark matter off two nucleons at once [22–24], or (a more radical modification) detection not of dark matter itself but of relativistic DM annihilation products [25]. Theories containing a large ensemble of (possibly unstable) dark matter states have been considered [26–29], as have theories in which only a small fraction of dark matter enjoys a richer set of interactions [30–33]. All of this theoretical exploration has helped to broaden our sense of what realistic theories of dark matter can be, pointing the way to new signatures that can be tested experimentally.

Our goal in this paper is to explore yet another modification of the standard picture of how dark matter interacts with other particles. Specifically, we will study dark matter interactions that are mediated by generic operators of arbitrary scaling dimension (consistent with unitarity bounds), which can be thought of as the exchange of a continuum of light states. Schematically, we would like to think about Lagrangians of the form

$$\mathcal{L} = \bar{\chi}\Gamma\chi\mathcal{O}_{\rm med} + \bar{\psi}\Gamma\psi\mathcal{O}_{\rm med}, \tag{1}$$

where $\bar{\chi}\Gamma\chi$ stands in for any dark matter bilinear operator and $\bar{\psi}\Gamma\psi$ for a Standard Model bilinear and $\mathcal{O}_{\rm med}$ is some "mediating operator". The precise technical meaning of the statement that a continuum of states is exchanged is that the momentum-space

* Corresponding author at: Theory Division, CERN, CH-1211 Geneva 23, Switzerland.
E-mail addresses: andrey.katz@cern.ch (A. Katz), mreece@physics.harvard.edu (M. Reece), sajjad@physics.harvard.edu (A. Sajjad).

http://dx.doi.org/10.1016/j.dark.2016.01.002

two-point function $\langle \mathcal{O}_{\rm med}(q)\mathcal{O}_{\rm med}(-q)\rangle$ has a branch cut extending down to momenta well below the threshold momentum exchange giving rise to a signal in the experiment, $|q| \ll q_{\rm exp}$ (and furthermore that the spectral weight is spread out along the branch cut rather than being concentrated near a single narrow peak). Cases where $\mathcal{O}_{\rm med}$ is a single light or heavy particle are well-studied, but the general case where it represents the exchange of a continuum of light states has received little attention. Such couplings to a continuum of states have appeared in the phenomenological literature in various guises, e.g. in the RS2 setup [34] or the literature on "unparticles" [35,36], but (perhaps surprisingly) has been mostly absent from explorations of how dark matter can interact with the Standard Model.

Let us mention here some related work in the literature. The possibility that direct detection could proceed through a continuum of states which would modify the effective nonrelativistic potential $V(r)$ was briefly discussed in Section 2.2 of [1], but not developed at length. An unusual velocity dependence of dark matter annihilation from the Sommerfeld effect due to exchange of a continuum of states was explored in [37]; related work neglecting the Sommerfeld effect appeared in [38]. Finally, a related scenario involving a Randall–Sundrum realization of a tower of light mediators was studied in [39–43].

The outline of this paper is as follows. In Section 2 we describe our setup in detail. In particular, we briefly review the CFT formalism that we use in our calculations and describe possible ways to model a mass gap. We show that the direct detection rates are almost not affected by our assumptions about the modeling of the mass gap. We also briefly address basic cosmological concerns related to our scenario. In Section 3 we study continuum mediators coupling to the SM Higgs portal [44–48]. It is a simple illustration of the general idea, but we find that there is not a viable parameter space for the sort of direct detection signal we are interested in. In Section 4 we analyze the DM direct detection and collider constraints in the case when the DM–nucleus interaction is mediated via an antisymmetric tensor operator which couples to the SM via the hypercharge portal [49,50]. This case realizes interesting continuum-mediated phenomenology in a parameter space compatible with various constraints. Finally in the last section we conclude. Some technical details are relegated to the Appendix.

2. The scenario: mass scales and kinematics

2.1. The basic picture

The majority of models of dark matter–baryon scattering considered so far take one of two forms:

Light particle mediator:

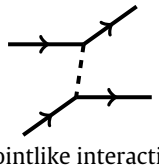

$$= J_\chi(p, p-q)\frac{1}{q^2}J_{\rm SM}(k, k+q). \tag{2}$$

Pointlike interaction:

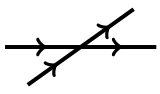

$$= J_\chi(p, p-q)J_{\rm SM}(k, k+q). \tag{3}$$

In position space, these correspond to potentials $V(r) \propto 1/r$ and $V(r) \propto \delta^{(3)}(\vec{r})$, respectively. (These are point-particle idealizations and should be appropriately convolved with the nuclear form factor and, if it exists, dark matter form factor.) We could also consider the case of a massive mediator with mass $m \sim q$, which would correspond to a Yukawa potential interpolating between these two extremes. In this paper, we consider a different scenario, in which we exchange a continuum of light modes. One way to think of this is as the result of coupling to states of multiple light particles:

Continuum mediator:

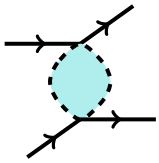

$$= J_\chi(p, p-q)\left(\frac{1}{q^2}\right)^\alpha J_{\rm SM}(k, k+q). \tag{4}$$

Here the scale-invariant factor of $(1/q^2)^\alpha$ is a stand-in for more general possible behavior of the intermediate continuum. In the simplest case, we could consider just a loop of two light, non-interacting particles. More generally, the continuum could consist of multiple particles that are themselves interacting, as suggested by the shaded region in the figure. These interactions could give the operator $\mathcal{O}_{\rm med}$ an anomalous dimension, and in the strong-interaction limit could render any simple particle interpretation unreliable.

The examples that we have written above involve a very important *factorization* property, which will apply to all of the models that we consider. Namely, the amplitude for dark matter–baryon scattering is a product of three factors:

- A Standard Model current or "portal". At the microscopic level, this may involve quarks or gluons. In a realistic direct detection calculation, the coupling is to *nuclei*, and so this piece of the amplitude in general involves a nuclear form factor describing the way that protons and neutrons are distributed within the nucleus. Such form factors are conveniently calculated with the code of [4].
- A dark matter current. Generally this is taken to be simpler than the Standard Model current, since dark matter is treated as an elementary particle. However, more generally, dark matter itself could have a form factor (see e.g. [18,51–53]).
- The propagation of the mediator. In the case of a contact interaction, this factor is simply 1. For a massless particle, it is $1/q^2$, corresponding to a long-range force. For this paper, we will take it to be of the form $1/(q^2)^\alpha$ (motivated by scale invariance) or more generally $1/(q^2 - m^2)^\alpha$ (which, as we will discuss below, is a crude but useful toy model for a mass gap).

Importantly, the propagation of the continuum mediator that we consider will always simply have the effect of rescaling well-understood calculations in the literature by simple functions of q^2. It never requires any new nuclear form factors, for instance. Furthermore, the dark matter and Standard Model currents may be in nontrivial representations of the Lorentz group, but the effect of the mediator will always resemble rescaling the result of a contact interaction by a Lorentz scalar function of q^2. In the case where the mediator has spin and its propagator may involve complicated tensor structures, this is not entirely obvious. We work out the details for an antisymmetric tensor mediator that mixes with the electromagnetic field strength in the Appendix, showing that the amplitude is a simple product of known amplitudes for electric or magnetic dipole moments and a power law in $-q^2$ for a general scale-invariant mediator.

2.2. A cosmological concern

The simplest realization of continuum exchange is to couple dark matter and the Standard Model to an operator in an infrared-conformal sector [34,35]. However, this is potentially cosmologically dangerous, because a conformal sector behaves as dark radiation and is subject to cosmological bounds due to

its effect on the expansion rate of the universe [54]. These are usually quoted as constraints on the number of "effective neutrino species", $N_{\rm eff}$, from BBN ($\Delta N_{\rm eff} < 1.44$ at 95% confidence [55]) and the CMB ($N_{\rm eff} = 3.15 \pm 0.23$ from Planck combined with other data [56]). If dark matter couples to dark radiation, these constraints can change in various ways depending on the form of the coupling [57–60], but they remain quite stringent. The safest way to avoid these bounds is if our continuum of particles does not extend all the way down to zero mass and develops a mass gap; if the particles become nonrelativistic before BBN, they are no longer dark radiation from the viewpoint of cosmological bounds. For instance, our approximately conformal sector could confine at a scale of at least a few MeV. This mass means that during BBN, the continuum of modes behaves as dark matter rather than dark radiation. We can also arrange that, after acquiring a mass, the continuum states simply decay before BBN, dumping their energy into the Standard Model plasma. For instance, if they couple to the Standard Model through dimension-six operators suppressed by a scale Λ, they can have a lifetime

$$\tau \sim \frac{\Lambda^4}{m^5} \sim 7 \times 10^{-7}\ \text{sec} \left(\frac{\Lambda}{100\ \text{GeV}}\right)^4 \left(\frac{10\ \text{MeV}}{m}\right)^5, \tag{5}$$

easily decaying before BBN (although stable on collider timescales). More refined estimates can be done for the particular models we discuss. In the particular case of the hypercharge portal, we will discuss such estimates further in Section 4.2. It is also possible that deviations from thermal equilibrium just before BBN could assist in circumventing the dark radiation bounds even if there is no mass gap (or the mass gap is much smaller than the BBN scale) [61].

2.3. The direct detection scale meets the BBN scale

Direct detection experiments search for nuclear recoil events. If a nucleus of mass m_N recoils with kinetic energy E_R, the momentum transfer is $q = \sqrt{2 m_N E_R}$ and the incoming dark matter velocity must have been at least $v_{\rm min} = \frac{q}{2\mu}$ where μ is the dark matter–nucleus reduced mass. A typical dark matter velocity in the galactic halo is $\bar{v} = 220$ km/s, which (taking $\mu = 100$ GeV for reference) can impart at most a momentum transfer of $q \approx 147$ MeV. A low-threshold nuclear recoil might be taken as, for instance, $E_R = 2$ keV for a silicon nucleus of mass ≈ 26 GeV [62], corresponding to about a 10 MeV momentum transfer. Thus, the range of momentum transfers that are relevant for direct detection might be roughly construed as

$$10\ \text{MeV} \lesssim q \lesssim 400\ \text{MeV}, \tag{6}$$

with the typical momentum transfer of interest in the middle of this range and the exact details depending on the particular experiment. LUX, for instance, studies nuclear recoils in xenon between about 3 and 25 keV [63], corresponding to 27 MeV $\lesssim q \lesssim$ 78 MeV.

From these estimates we see that, if the continuum of modes mediating scattering acquires a mass gap $m \approx 10$ MeV in order to avoid dark radiation bounds during BBN, this mass will be a subdominant correction to the two-point function $\langle O_{\rm med}(q) O_{\rm med}(-q)\rangle$ at the values of q that are most relevant for direct detection. The "mass-gap" solution to the BBN bound suffers from a coincidence problem: we have no explanation for why the gap should fall in the relatively small interval between the temperatures relevant for BBN and the momenta relevant for direct detection. (Particular models may offer solutions, but no general solution is apparent.) But if we *assume* that $T_{\rm BBN} \lesssim m \lesssim q_{\rm exp}$, we have interesting direct detection phenomenology while dodging the cosmological bound. If we prefer to avoid accidental coincidences of mass scales, we can always pursue the more elaborate nonthermal cosmologies alluded to above to allow for much smaller m.

2.4. The conformal limit

Now that we have argued that we can at least approximately neglect masses over the range of momenta relevant for direct detection experiments, let us introduce the formalism we will use throughout most of the paper, which assumes the conformal field theory limit. To outline the basic formalism and the assumptions we rely on, we will discuss one of the simplest cases we can consider. Namely, $\mathcal{O}_{\rm med}$ is a scalar operator of dimension d, coupling to the Standard Model through the Higgs portal [44,45] and to a Dirac fermion dark matter particle χ through a scalar bilinear:

$$\mathcal{L} = \frac{c_h}{\Lambda^{d-2}} H^\dagger H \mathcal{O} + \frac{c_0}{\Lambda^{d-1}} \mathcal{O}\bar{\chi}\chi. \tag{7}$$

(We now drop the subscript "med" for convenience.) The first term is marginal if $d = 2$; we could imagine generating a scalar operator with $d \approx 2$ in various ways, including as a fermion bilinear $\bar{\psi}\psi$ near the edge of the conformal window in a QCD-like theory [64]. For most of the discussion in this paper, the only information that we need about the operator $\mathcal{O}$ is its two-point function, to which we assign a simple expression in position space. For future use, we also quote the result for an antisymmetric tensor operator:

$$\langle \mathcal{O}(x)\mathcal{O}(0)\rangle = \frac{c_{\mathcal{O}}}{4\pi^2 |x|^{2d}}, \tag{8}$$

$$\left\langle \mathcal{O}_{\mu\nu}(x)\mathcal{O}^{\lambda\sigma}(0)\right\rangle = \frac{c_{\mathcal{O}}}{4\pi^2 |x|^{2d}} I^{\lambda}_{[\mu}(x) I^{\sigma}_{\nu]}(x),$$

$$\text{where } I_{\mu\nu}(x) = g_{\mu\nu} - 2\frac{x_\mu x_\nu}{x^2}. \tag{9}$$

Unitarity requires $d \geq 1$ for the scalar case and $d \geq 2$ for the antisymmetric tensor. In momentum space the two-point functions acquire extra prefactors:

$$\begin{aligned}\langle \mathcal{O}(-q)\mathcal{O}(q)\rangle &\equiv \int d^4x\, e^{iq\cdot x} \langle \mathcal{O}(x)\mathcal{O}(0)\rangle \\ &= \frac{\Gamma(2-d)}{4^{d-1}\Gamma(d)} c_{\mathcal{O}} (-q^2)^{d-2}, \end{aligned} \tag{10}$$

$$\begin{aligned}\left\langle \mathcal{O}_{\mu\nu}(q)\mathcal{O}^{\lambda\sigma}(-q)\right\rangle &= -\frac{\Gamma(3-d)}{4^{d-1}\Gamma(d+1)} c_{\mathcal{O}} \left(-q^2\right)^{d-2} \\ &\quad \times \left(g^{[\lambda}_{\mu} g^{\sigma]}_{\nu} - \frac{2}{q^2} q_{[\mu} q^{[\lambda} g^{\sigma]}_{\nu]}\right). \end{aligned} \tag{11}$$

In both these expressions $c_{\mathcal{O}}$ is a normalization constant and we will further take it to be 1 to simplify the calculations. We work in a mostly-minus metric so that the branch cut arises at physical timelike momentum $q^2 > 0$. Because we will mostly use the momentum-space expression, one might wonder why we do not assign it the simple coefficient $c_{\mathcal{O}}$ and shift the unpleasant Gamma functions into the less-used position space answer. The reason is that we would like smooth behavior of answers near integer dimension: if $d \approx n + \epsilon$, then

$$(-q^2)^{n-2+\epsilon} \approx (-q^2)^{n-2} \left(1 + \epsilon \log(-q^2) + \cdots\right), \tag{12}$$

in which it turns out that the leading term is removed by contact terms and the $\log(-q^2)$ piece is physical. In fact, the $\log(-q^2)$ factor is, for integer dimension operators, the source of the branch cut corresponding to a continuum of physical states. It appears that it would vanish in the $\epsilon \to 0$ limit, but this is compensated by a $\frac{1}{\epsilon}$ from a pole in the prefactor $\Gamma(2-d)$, which we therefore want to keep. (Further discussion of such subtleties may be found in Ref. [36].)

The next subtlety to discuss is the meaning of the scale Λ. We could imagine that this is a true cutoff: local field theory begins at the scale Λ, at which point operators already exist with unusual

scaling dimensions, and we are simply given the Lagrangian. But, especially since the values of Λ that we can probe will not be far beyond the TeV scale, it seems more likely that the physics is established at some higher energy scale, possibly in terms of weakly-coupled elementary fields, and RG running toward strong coupling leads to the development of large anomalous dimensions and CFT-like behavior. In this case Λ may be a combination of other underlying mass scales.

We will not dwell at length on UV completions in this paper, but let us elaborate on this point. Say that the operator $\mathcal{O}$ has a nontrivial scaling dimension, perhaps $d = 2 + \epsilon$. Then we might parametrize its coupling to the Standard Model as $\frac{1}{\Lambda^\epsilon} h^\dagger h \mathcal{O}$. This is an unusual expression, and especially if Λ is a relatively low scale (say, 10 TeV), we should expect that there is dynamics lurking behind it. Perhaps, for example, at some energy Λ_0 this originated in a dimension-5 interaction of weakly-coupled fields, $\frac{1}{\Lambda_0} h^\dagger h \bar{\psi}\psi$, and then some other interactions at strong coupling drove the operator $\bar{\psi}\psi$ to have a nontrivial scaling dimension. If these interactions became important at a scale $M \ll \Lambda_0$, then we should match $\bar{\psi}\psi \to M^{1-\epsilon}\mathcal{O}$, and we infer that the effective scale Λ suppressing the operator at low energies is $\Lambda = \Lambda_0(\Lambda_0/M)^{\frac{1-\epsilon}{\epsilon}} \gg \Lambda_0$. Meanwhile, depending on the UV completion, perhaps there were also contact interactions *directly* linking the Higgs to dark matter at the scale Λ_0. The fact that $\Lambda \gg \Lambda_0$ thus raises two concerns:

- If $M \ll \Lambda_0 \ll \Lambda$, then we either have to make Λ quite large (suppressing our signals) or squeeze a lot of dynamics into energies near the weak scale (possibly giving rise to new constraints).
- If other baryon–dark matter interactions are suppressed by Λ_0 rather than Λ, they may give larger effects than those mediated by $\mathcal{O}$.

These concerns suggest to us that we should focus on cases where $\mathcal{O}$ is an operator of low dimension. If $\mathcal{O}$ mediates a long-range force, which is to say, if the effective amplitude for scattering mediated by $\mathcal{O}$ is proportional to a *negative* power of $-q^2$, then the powers of (Λ_0/Λ) that tend to suppress the effects of $\mathcal{O}$-mediated exchange may be overcome by powers of the large ratio $\Lambda^2/(-q^2) \gg 1$. Precisely because direct detection operates at low momentum transfer, the effects that we are studying may be observable.

Given any effective continuum-mediated model, it would be interesting to follow this logic through more carefully in concrete UV completions. For now, however, we simply take away the general lesson that continuum-mediated scattering is most likely to be observable when the amplitude involves negative powers of $-q^2$, and is potentially subdominant (though this is UV-dependent) to contact interactions when this is not the case.

2.5. Implications of the mass gap

For a free field, the change from massless to massive is straightforward: we replace the propagator i/q^2 with $i/(q^2 - m^2)$. (For higher spin fields there are also modifications to the tensor structure in the numerator.) But for generic operators, there is no universal prescription for how the mass gap appears in the two-point function. The spectral function will be zero below the threshold mass m, and nonzero above it, asymptoting to the gapless answer; but the near-threshold behavior could be quite complicated. For confining gauge theories, for instance, we have no analytic tools to compute the precise spectral function. Nonetheless, it is useful to have some simple examples to make more quantitative statements about to what extent a $\sim$10 MeV mass gap can alter simple scale-invariant predictions for direct detection rates. For direct detection, we are interested in spacelike values $q^2 < 0$, because q is a momentum transfer; this helps to protect our answers from extreme sensitivity to the near threshold behavior, since the threshold and any associated peaks in the spectral function are at $q^2 > 0$.

Let us explore how sensitive the answer is to different models of the mass gap. The simplest conceivable toy model is to replace $(-q^2)^\alpha \to (m^2 - q^2)^\alpha$ [65]. Other toy models can come from loops of massive particles or from confining gauge theories or extra dimensions. For simplicity and concreteness, let us focus on the case of dimension 2 scalar operators, for which the CFT two-point function is (up to normalization) simply $\log(-q^2)$. The simple toy model, then, would replace this with $\log(m^2 - q^2)$. One way to obtain a dimension 2 scalar is as a product of two free scalars; in this case the spectral function arises from a loop integral. If we give the free scalar a mass m_0, we introduce a branch cut for the two-particle operator at the threshold $m = 2m_0$, and find that $\Pi(q^2) \propto \int_0^1 dx\, \log(-x(1-x)q^2 + \frac{1}{4}m^2) + 2$. (We shift the result by two so the asymptotics matches $\log(-q^2)$ at $-q^2 \to \infty$.) A third toy model motivated by the RS2 interpretation of the conformal two-point function is to imagine inserting an infrared brane or "hard wall" to produce a mass gap, as in RS1 [66], or approximately in confining gauge theory at large 't Hooft coupling (see e.g. [67]). We can then compute

$$\Pi(q^2) = \frac{J_0(\sqrt{q^2/q_0^2})\log(q^2/q_0^2) - \pi Y_0(\sqrt{q^2/q_0^2})}{J_0(\sqrt{q^2/q_0^2})}. \tag{13}$$

If $x_1 \approx 2.404$ is the first root of $J_0(x)$, then we choose $q_0^2 = m^2/x_1^2$ to obtain a mass threshold m. For this model the spectral function is a sum over poles, as in a large-N gauge theory. In a finite-N theory all of these poles acquire a width; we can approximate this effect on the spectral function by studying the large-N answer slightly away from the real axis, effectively smearing out the narrow states: $\rho_\Delta(s) = \frac{1}{2i}(\Pi(s+i\Delta) - \Pi(s-i\Delta))$ [68,69]. An alternative large-N model, perhaps more representative of real QCD (or other theories with small UV 't Hooft coupling), is the digamma function [69–71]: $\Pi(q^2) = \psi(-q^2 + m^2)$, which has its first pole at m^2 and asymptotes to $\log(-q^2)$ for large negative q^2.

These four toymodels are illustrated in Fig. 1. The right-hand panel shows the smeared spectral function, which varies from a step function (in the simple $\log(-q^2 + m^2)$ ansatz) to a smooth curve that turns on (the loop of massive scalars) to wildly bumpy curves characteristic of confining large-N theories with many narrow resonances. Despite these dramatically different spectral functions, the behavior for *spacelike* momentum, as shown in the left-hand plot, is qualitatively similar in every case. In particular, the corrections to the asymptotic conformal answer when $-q^2 \gg m^2$ are very small. This gives us confidence that the behavior of the direct detection cross section can be approximated with the simplest toy ansatz, $q^2 \to q^2 - m^2$, even without a detailed model for the origin of the mass gap. Such an ansatz will certainly lead to the correct qualitative physics, and will be quantitatively reasonable unless we probe too close to $|q^2| \approx m^2$.

Although we have only given examples for the special case $d = 2$, we expect that similar results would be obtained for other dimensions. (Hard and soft wall extra dimensional theories can produce results for arbitrary operator dimension by varying the bulk mass; generalizing the loop ansatz in a well-motivated way appears more difficult.)

3. Higgs portal

First, let us briefly analyze the higgs portal for the continuum-mediated Dirac fermion DM. Because it involves a scalar operator, this case is formally the simplest. Although we will immediately

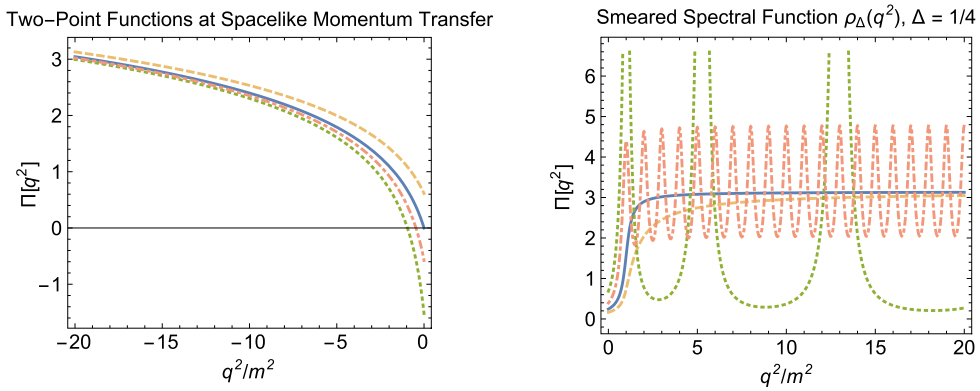

Fig. 1. Four toy models for a mass gap in the two-point function of a dimension-2 scalar operator. In every case, $\Pi(q^2) \to \log(-q^2)$ in the spacelike region $q^2 \ll 0$. The four models are similar at spacelike momentum (left) but differ greatly for timelike momentum (right). Solid blue: the simple replacement $\log(-q^2 + m^2)$. Dashed orange: the result for a loop of free massive scalars. Dotted green: the Randall–Sundrum or "hard-wall" ansatz, characteristic of confinement at large 't Hooft coupling. Dot-dashed red: the digamma function, a toy model of QCD-like confinement. (For interpretation of the references to color in this figure legend, the reader is referred to the web version of this article.)

see this portal is excluded by the current data, at least within the standard cosmology, some of the results that we get here are relevant for a much more motivated hypercharge portal. The coupling of the mediator to the SM that we assume in the Higgs portal is

$$\mathcal{L} = c_H \frac{H^\dagger H \mathcal{O}}{\Lambda^{d-2}}, \tag{14}$$

with d being a scaling dimension of the scalar operator $\mathcal{O}$, whose critical dimension is 1. The most generic coupling that one could write down to the fermionic DM is

$$\mathcal{L} = c_0 \frac{\mathcal{O}\bar{\chi}\chi}{\Lambda^{d-1}} + \tilde{c}_0 \frac{\mathcal{O}\bar{\chi}\gamma^5\chi}{\Lambda^{d-1}}. \tag{15}$$

Note that a priori the scales Λ in Eqs. (14) and (15) can be very different from one another. We absorb these differences in the couplings c_0 and c_H which are not necessarily $\mathcal{O}(1)$.

As we claimed in Section 2 these interactions can be reduced to the standard fermionic higgs portal with a q^2-dependent coefficient. This approach is very similar to the approach that we are taking in the hypercharge portal scenario, where we will define q^2-dependent moments. The effective higgs portal is

$$\mathcal{L} = c_{\rm eff}(q^2) \frac{|H|^2 \bar{\chi}\chi}{\Lambda} + \tilde{c}_{\rm eff}(q^2) \frac{|H|^2 \bar{\chi}\gamma^5\chi}{\Lambda} \tag{16}$$

with

$$c_{\rm eff} \equiv \frac{c_H c_0 \Gamma(2-d)}{4^{d-1}\Gamma(d)} \left(\frac{-q^2}{\Lambda^2}\right)^{d-2}. \tag{17}$$

The expression for $\tilde{c}_{\rm eff}$ is identical to that for $c_{\rm eff}$ up to an obvious change $c_0 \to \tilde{c}_0$. It is very easy to qualitatively understand what would be the implications of this kind of higgs portal on direct detection. The momentum-dependent coupling $c_{\rm eff}(q^2)$ would translate into an effective dependence of the recoil spectrum on q^2, inducing an effective form factor, which has nothing to do with either nuclear or dark matter form factors, but rather arises because of the unusual properties of the mediator.

Unfortunately, higgs portal continuum-mediated DM is not viable because of the immediate clash between the induced mass-gap in the mediator sector and the cosmological constraints. Interestingly, for any $d < 4$, Eq. (14) induces a mass gap in the mediator sector which is

$$m_{\rm gap} = \left(\frac{c_H v^2}{\Lambda^{d-2}}\right)^{\frac{1}{(4-d)}}. \tag{18}$$

Of course if this mass gap is too small we can always assume extra sources, which might generate an additional mass gap. However, it is difficult to see how one would significantly reduce this induced mass gap without very severe fine-tuning. At first glance the automatic presence of a mass gap is *good* from the point of view of satisfying BBN constraints; the problem is that the model is too predictive, implying too long a lifetime for a given mass gap.

As we will immediately see the induced mass gap (18) is too large in those regions of parameter space where we can satisfy the cosmological constraints. As explained in Section 2, the lightest particle in the mediation sector with a mass of order $m_{\rm gap}$ should decay faster than one second. Assuming that this particle is a scalar s with a mass m_s we can write down its matrix element as

$$\langle 0|\mathcal{O}|p\rangle = \xi_s m_s^{d-1} e^{ip\cdot x}. \tag{19}$$

In this expression ξ_s is an unknown $\mathcal{O}(1)$ constant, that we will take to one in our further estimates. Therefore the term (14) induces mixing between the scalar s and the physical h, which the scalar s can decay through. Kinematically, only decays $s \to e^+e^-$ and $s \to \gamma\gamma$ are allowed and their rates are

$$\Gamma(s \to e^+e^-) = \frac{2c_H^2 v^2 m_s^{2d-2}}{\Lambda^{2d-4} m_h^4} \Gamma_{h\to e^+e^-}(m_s) \tag{20}$$

$$\Gamma(s \to \gamma\gamma) = \frac{2c_H^2 v^2 m_s^{2d-2}}{\Lambda^{2d-4} m_h^4} \Gamma_{h\to\gamma\gamma}(m_s), \tag{21}$$

where $\Gamma_{h\to XX}(m_s)$ stands for the higgs partial decay widths *if it had a mass* m_s*, rather than* m_h. In the relevant range of s masses, 1 MeV $< m_s <$ 100 MeV one can easily see that the $\gamma\gamma$ channel is completely subdominant and disregard it. The decay to the electron pairs is the only viable decay channel of s, and because the rate is suppressed by the electron Yukawa squared, the constraints are not very easy to satisfy. In practice the constraint $\tau_s < 1$ sec translates to the following bound:

$$c_H^2 \left(\frac{\Lambda}{100\ \text{GeV}}\right)^2 \left(\frac{m_s}{10\ \text{MeV}}\right) \left(\frac{m_s}{\Lambda}\right)^{2d-2} > 2 \times 10^{-11}. \tag{22}$$

It is easy to see that one cannot satisfy this constraint and the demand $m_{\rm gap} \lesssim 50$ MeV simultaneously. The latter suggests that $d > 3$ for any phenomenologically interesting range of the scale Λ. The former demands that $d \lesssim 2.34$ for $\Lambda \sim 1$ TeV, and even slightly smaller values of d for higher values of Λ.

Of course, the constraint on the decay time of the lightest narrow state can be circumvented if we assume non-standard cosmology, but we still view the constraints on this scenario as

not appealing and further concentrate on the hypercharge portal, which is much more promising.[1] Precisely because it does not involve a scalar operator, the coupling to the Standard Model in the hypercharge portal case does not automatically deform the CFT and produce a mass gap, so masses and lifetimes are no longer closely linked and there will be a larger viable parameter space to explore.

4. Hypercharge portals

4.1. Portal and recoil spectrum

We start from studying the hypercharge portal where the hypercharge field strength couples to an antisymmetric operator,

$$\mathcal{L} = \frac{c_B}{\Lambda^{d-2}} B_{\mu\nu}\mathcal{O}^{\mu\nu}. \tag{23}$$

The critical dimension of the antisymmetric tensor is 2, so the dimension of this operator is always bigger than or equal to 4. This is a unique portal in the SM, because it allows coupling of the BSM bosonic particles to the SM with an operator of dimension 4.[2] Moreover, in the context of the DM, it is the only low-dimension operator which allows couplings of the DM to the SM which are not suppressed by the masses of heavy mediators: EW bosons, Higgs or BSM particles (e.g. Z').

The event rate and the total cross sections in the direct detection experiment strongly depend on the coupling of the antisymmetric tensor $\mathcal{O}_{\mu\nu}$ to the DM particles. Hereafter we will only consider operators with dimensions not higher than 6 in the limit $d[\mathcal{O}_{\mu\nu}] \to 2$. With this restriction, and assuming fermionic dark matter one can straightforwardly write down three different coupling of the DM to this operator:

$$\mathcal{L} = \frac{c_2}{\Lambda^{d-1}} \mathcal{O}_{\mu\nu}\bar{\chi}\sigma^{\mu\nu}\chi \tag{24}$$

$$\mathcal{L} = \frac{\tilde{c}_2}{\Lambda^{d-1}} \mathcal{O}_{\mu\nu}\chi\sigma^{\mu\nu}\gamma^5\chi \tag{25}$$

$$\mathcal{L} = \frac{\bar{c}_2}{\Lambda^{d}} \partial^{\nu}\mathcal{O}_{\mu\nu}\bar{\chi}\gamma^{\mu}\gamma^5\chi. \tag{26}$$

Because of the structure of these operators, which are identical to the magnetic dipole moment (MDM), the electric dipole moment (EDM) and to the anapole by replacing $\mathcal{O}_{\mu\nu} \to F_{\mu\nu}$, we will loosely refer to each of these options as magnetic, electric and anapole hypercharge portals respectively. As in the previous sections, we do not necessarily assume that the couplings c_B, c_2, $\tilde{c}_2$ and $\bar{c}_2$ are order one.

As we briefly outline in Section 2 and prove in the Appendix, one can reduce each of these couplings to the effective dipole/anapole coupling of the DM to the SM photon, reweighted by an appropriate power of $-q^2$, where the latter is the momentum exchanged between the DM and the nucleus in the scattering process. Therefore, each of these terms yields an effective (momentum-dependent) DM dipole moment, which depends on an appropriate power of $-q^2$. The explicit calculation gives the following effective magnetic dipole moment for the operator (24):

$$\mu_{\rm mag} = \frac{c_B c_2 \cos\theta_W}{\Lambda^{2d-3}} \frac{\Gamma(3-d)}{4^{d-2}\Gamma(d+1)} \left(-q^2\right)^{d-2}. \tag{27}$$

For the EDM and the anapole hypercharge portals we get exactly the same expression for the effective moment with an obvious replacement $c_2 \to \tilde{c}_2$ for the EDM and $c_2 \to \bar{c}_2$, $\Lambda^{2d-3} \to \Lambda^{2d-2}$ for the anapole moment.

Because all the effective moments depend in a non-trivial way on the momentum transfer q^2, we expect that the differential event rates dR/dE_R will be modified compared to the "standard" DM dipole/anapole scenario. One can refer to the factor $(q^2)^{d-2}$ as an effective DM form factor. However this form factor arises because of the non-trivial dynamics in the mediation sector, rather than non-trivial structure of the DM. Of course these effective DM form-factors multiply the nuclear form-factor in the direct detection picture, yielding distinctive event distributions in the direct detection experiments.

It is also worth noticing that the effective DM form-factors will be further modified compared to the perfect CFT limit by the mass gap effects. If this mass gap is not too far away from the BBN limit, namely $m_{\rm gap} \sim \mathcal{O}(1\ldots 10)$ MeV, this modification is mostly important in the low-energy recoil regime. Therefore we expect stronger modifications for the lighter elements, e.g. fluorine and oxygen, while the heavy elements like xenon might be only very weakly sensitive to the mass gap effects.

To illustrate these points we show the expected rate distributions dR/dE_R assuming scattering on both ^{131}Xe and ^{19}F for both electric and magnetic dipoles on Fig. 2.[3] These figures are meant to illustrate only the shape of the curve, and so have arbitrary normalization. The differences between the distributions are clearly seen. We further show the rates if the conformal invariance is broken by mass gaps $m_{\rm gap} = 15$ MeV and $m_{\rm gap} = 40$ MeV in Fig. 3. In this case, the overall normalization remains arbitrary but the relative normalization of curves on the same plot is important, showing how the mass gap suppresses the overall rate in a momentum-dependent manner. To model the mass gap here we use the most naive model, namely we replace $-q^2 \to (-q^2 + m_{\rm gap}^2)$. Because the momentum transfer is spacelike we assume very little possible difference between different ways to model this effect (see Section 2.5 for details). As we see the effect is minor or very minor for scattering on ^{131}Xe, however it is as expected much more pronounced for scattering on ^{19}F.

From here we can immediately calculate the total cross sections and the differential event rates in the direct detection experiments. Of course, there are differences between the electric dipole on one side and magnetic dipole/anapole on another side. While the cross section of the former is enhanced by q^{-1} in the $d[\mathcal{O}_{\mu\nu}] \to 2$ limit, the cross sections of the anapole are completely regular and behave as q^0 in this limit. The MDM cross section is technically also enhanced by q^{-1} and the total cross-section diverges in the deep IR, this term is suppressed by the transverse velocity, translating to the non-relativistic operator $\frac{i}{q^2}\vec{S}_\chi \cdot (\vec{q}\times\vec{v})$. Therefore, we expect to get much bigger cross sections in the EDM case than in the other cases for the same values of Λ and d. The cross sections have been calculated in multiple previous works

[1] Another potential way to circumvent the constraints on the higgs portal would be speeding up the decay of the scalar s by introducing new couplings, which do not necessarily have anything to do with the DM, *e.g.* $\mathcal{O}F^2_{\mu\nu}$. However this is not the most minimal scenario and these types of couplings come with their own constraints. We relegate the analysis of these non-minimal scenarios to future studies.

[2] Another unique portal which allows coupling of the BSM fermions to the SM with an operator of dimension 4 is the so-called "neutrino portal" *HL*. We will not consider the fermionic mediators in this paper, mainly because it is not easy to think about a scenario, where it would not spoil observed neutrino properties.

[3] In xenon experiments like LUX and Xenon100 one of course is sensitive to the nuclear responses of all the seven stable xenon isotopes, and not only to ^{131}Xe. We checked this explicitly, and the distributions that we show do not change significantly when all other isotopes are included. Therefore here for the illustration purposes we just use one isotope.

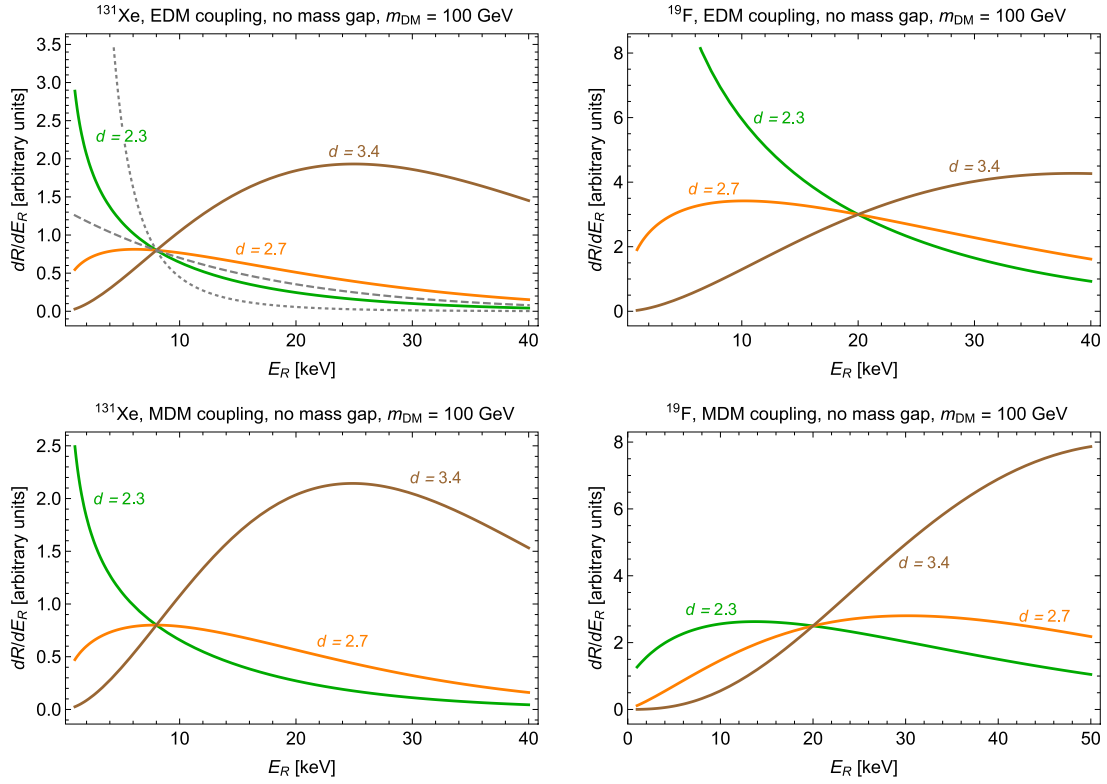

Fig. 2. Event rate in arbitrary units for electric-hypercharge (top panel) and magnetic-hypercharge (bottom panel) portals for different values of d. Green, orange and brown lines stand for $d = 2.3,\ 2.7,\ 3.4$ respectively. The curves have been artificially scaled to intersect at a single point, because the goal is to convey shape information only. The isotope ^{131}Xe is shown at left and ^{19}F at right. Notice that, due to different behavior of nuclear form factors, the shapes can be quite different for different atoms. To guide the reader's intuition for how these compare to more familiar scenarios, in the upper-left figure we also show the recoil spectrum arising from the standard contact operator coupling to mass ($\bar{\chi}\chi\bar{N}N$) as a dashed gray line and the same operator with a massless mediator ($\bar{\chi}\chi\bar{N}N/q^2$) as a dotted gray line. (For interpretation of the references to color in this figure legend, the reader is referred to the web version of this article.)

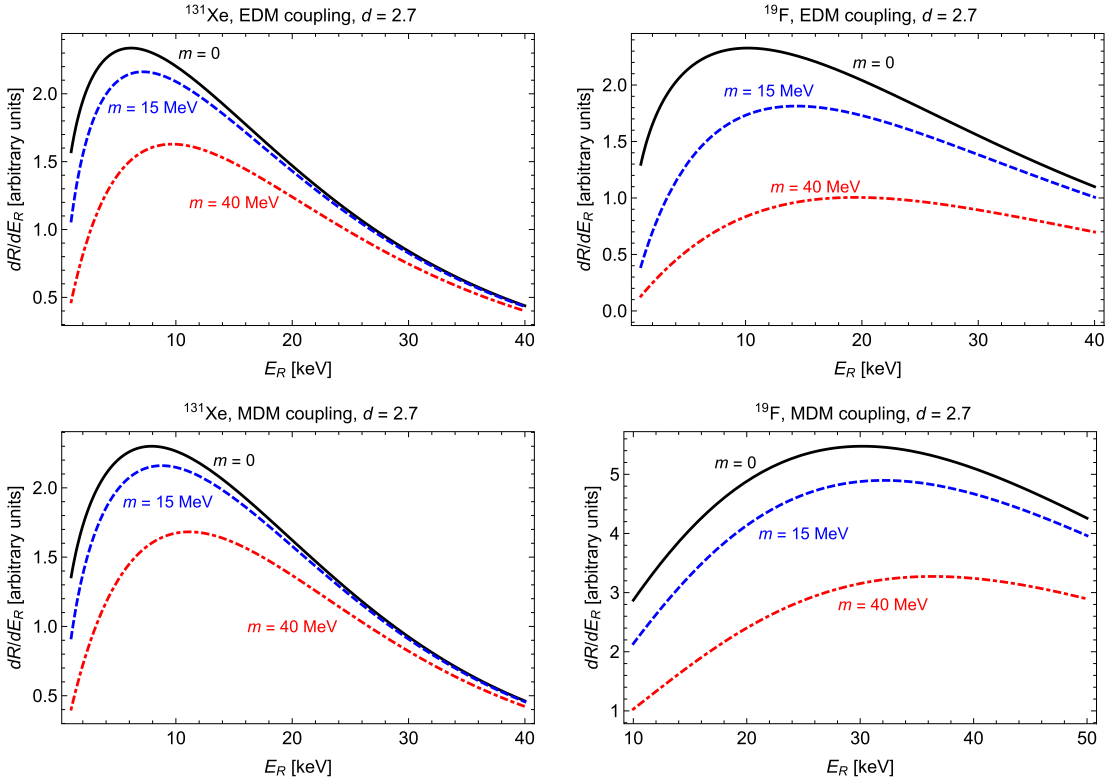

Fig. 3. Event rate in arbitrary units for electric-hypercharge (top panel) and magnetic-hypercharge (bottom panel) portals with and without mass gap. Black (solid), blue (dashed) and red (dot-dashed) lines stand for $m_{gap} = 0,\ 15,\ 40$ MeV respectively. We assume $d = 2.7$ on all these plots. (For interpretation of the references to color in this figure legend, the reader is referred to the web version of this article.)

on the dipole/anapole DM [72–76]. The EDM cross section can be calculated from integrating the following expression

$$\frac{d\sigma_{\rm EDM}}{d\cos\theta} = \frac{Z^2e^2}{4\pi v^2}\frac{\mu_{\rm el}^2(q^2(\cos\theta))}{1-\cos\theta} \tag{28}$$

which is of course divergent for $d = 2$, but finite for any other legitimate choice of d.

The expression for the MDM cross section is slightly more complicated, and includes both a finite dipole–dipole piece and a formally divergent dipole–charge radius interaction. The cross sections for these interactions are

$$\frac{d\sigma_{\rm MDM\text{-}charge}}{d\cos\theta} = \frac{e^2\mu_{\rm mag}^2(q^2(\cos\theta))Z^2}{4\pi} \times\left(\frac{1}{1-\cos\theta}-\frac{m_\chi}{(m_\chi+m_A)v^2}\right) \tag{29}$$

$$\frac{d\sigma_{\rm MDM-MDM}}{d\cos\theta} = \frac{\mu_Z^2\mu_{\rm mag}^2(q^2(\cos\theta))}{2\pi v^2}. \tag{30}$$

One can get total cross sections for the DM–nucleon scattering from integrating these expressions over $\cos\theta$. However, as we will explain later in Section 4.5, the direct detection experiments are sensitive to the effective cross sections, rather than "honest" total cross sections. Therefore, we will return to this question in Section 4.5 and get numerically the effective cross sections, taking into account the constraints on operator (23).

4.2. The BBN constraint

As we have mentioned in Section 2.2, we imagine that there is a mass gap for particles created by the operator $\mathcal{O}_{\mu\nu}$ and that these particles decay before BBN. First, let us suppose that the *only* particles we need to concern ourselves with are those created by $\mathcal{O}_{\mu\nu}$. Consider a vector particle V of mass m_V, which has a matrix element

$$\left\langle 0|\mathcal{O}_{\mu\nu}(x)|p,\epsilon\right\rangle = \xi_V m_V^{d-2}\left(\epsilon_\mu p_\nu - \epsilon_\nu p_\mu\right)e^{ip\cdot x}. \tag{31}$$

Here ξ_V is an order-one constant whose value can only be computed if we understand the detailed dynamics behind the mass gap.

Through the mixing of $\mathcal{O}_{\mu\nu}$ with hypercharge, the V particle can decay into charged Standard Model particles. In the mass range $m_V \sim 10$ MeV that is primarily of interest to us, the only kinematically accessible particles will be electrons since $m_{e^-} \approx 511$ keV. Neutrinos also carry hypercharge, but we are considering a process at energies below the Z boson mass for which a decay to neutrinos will carry extra m_V^2/m_Z^2 suppression in the amplitude. As a result, we are interested in computing the partial width for the decay $V \to e^+e^-$. This is closely analogous to the $\rho^0 \to e^+e^-$ process in QCD, which proceeds via kinetic mixing of the rho and the photon, or the frequently studied case of dark photons (e.g. [77]). The kinetic mixing of the V particle is

$$\frac{\epsilon_V}{2}V_{\mu\nu}F^{\mu\nu}, \quad \epsilon_V = 2c_B\xi_V\cos\theta_W\left(\frac{m_V}{\Lambda}\right)^{d-2}. \tag{32}$$

We compute

$$\Gamma(V\to e^+e^-) \approx \frac{4}{3}\xi_V^2c_B^2\alpha\cos^2\theta_W m_V\left(\frac{m_V}{\Lambda}\right)^{2d-4} \times\left(1+\frac{2m_e^2}{m_V^2}\right)\sqrt{1-\frac{4m_e^2}{m_V^2}}. \tag{33}$$

We require the lifetime $\tau(V\to e^+e^-) \lesssim 1$ s in order to avoid BBN constraints. This translates into a bound (dropping the phase space factors, which are negligible if $m_V \gg 1$ MeV):

$$\xi_V^2c_B^2\left(\frac{m_V}{\Lambda}\right)^{2d-4}\left(\frac{m_V}{10\text{ MeV}}\right) \gtrsim 9\times10^{-21}. \tag{34}$$

As expected, then, decay of the vector can easily happen before BBN when d is not too large. Alternatively, we can express the bound in terms of the effective mixing as

$$\epsilon_V \gtrsim 1.7\times10^{-10}\sqrt{\frac{10\text{ MeV}}{m_V}}. \tag{35}$$

We note that this estimate could be overly conservative: more detailed computations of constraints on dark photons from BBN and the CMB have found that smaller values of ϵ_V may be safe [78]. On the other hand, these studies have assumed a single dark photon with abundance determined from thermal equilibrium; in our case, there is a whole dark sector. Precise constraints may depend on the full model of the sector, but we will take our simple estimates to be the best guide available in the absence of a detailed model-dependent study.

The above constraint is the correct one if the only particles in the approximately scale-invariant sector are vectors, in which case they all decay directly through the mixing with hypercharge. On the other hand, familiarity with a range of examples of strongly-interacting theories tells us that often the lightest states are scalars or pseudoscalars. These could decay through other portals, like the Higgs portal—though as we noted above, the small value of the electron Yukawa suppresses decays through that portal. Alternatively, we could assume that the mixing between $\mathcal{O}_{\mu\nu}$ and hypercharge is the only coupling between this sector and the Standard Model. It does not permit a direct decay of a light scalar into Standard Model states. However, the scale-invariant sector will in general admit couplings of such a light scalar to heavier vectors, which in turn mix with the Standard Model. Suppose, then, that we have in addition to the vector V considered above a scalar S with mass $m_S < m_V$. We expect that the strong sector will contain couplings like

$$\mathcal{L}_{\rm eff} = \frac{\xi_{SVV}}{m_V}SV_{\mu\nu}V^{\mu\nu}, \tag{36}$$

where we assume that $m_S \sim m_V \sim m_{\rm gap}$ are all of the same order and ξ_{SVV} is an order-one number. This effective coupling allows the decay $S \to \gamma\gamma$ through two insertions of $V-\gamma$ mixing. We compute this decay width to be:

$$\Gamma(S\to\gamma\gamma) \approx \xi_{SVV}^2\xi_V^4\cos^4\theta_W c_B^4\left(\frac{m_V}{\Lambda}\right)^{4d-8}\frac{m_S^3}{4\pi m_V^2}. \tag{37}$$

Again, if we impose a $\tau \lesssim 1$ s constraint this leads to a bound:

$$\xi_{SVV}^2\xi_V^4c_B^4\left(\frac{m_V}{\Lambda}\right)^{4d-8}\left(\frac{m_S}{10\text{ MeV}}\right)^3\left(\frac{15\text{ MeV}}{m_V}\right)^2 \gtrsim 3.2\times10^{-21}. \tag{38}$$

Again, we can write this as a bound on the mixing

$$\epsilon_V \gtrsim 1.3\times10^{-5}\,\xi_{SVV}^{-1/2}\left(\frac{10\text{ MeV}}{m_S}\right)^{3/4}\left(\frac{m_V}{15\text{ MeV}}\right)^{1/2}. \tag{39}$$

In the alternative case that the lightest state is a pseudoscalar P, the logic is essentially identical with the modification that the effective coupling is of the type $PV_{\mu\nu}\tilde{V}^{\mu\nu}$. We take this to be a conservative bound on the constraint imposed by BBN on the hypercharge portal. Of course, if the lightest state really is a vector, we can use the safer bound from $V\to e^+e^-$.

In both cases, we see that the most obvious danger arises when $d \gg 2$. In that case the small ratio m_V/Λ is raised to a significant power and could potentially become small enough to cause problems. On the other hand, direct constraints tend to be strongest at small values of d, so we will carefully check whether the parameter space we consider below conflicts with these constraints. However, as we noted in Section 2.2, it is also possible that a nonstandard cosmological history can eliminate the problem even if these bounds are violated.

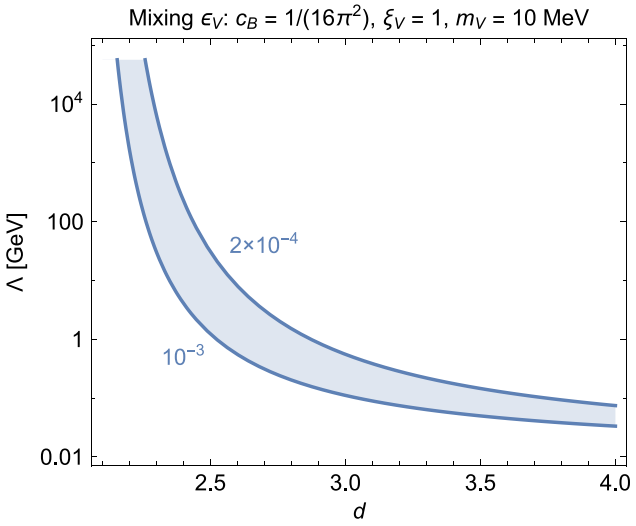

Fig. 4. Region of parameter space allowed by the inequality (40) in blue. We have fixed $c_B = \frac{1}{16\pi^2}$ (representative of a one-loop factor), $\xi_V = 1$, and $m_V = 10$ MeV, and plot the band of allowed mixing ϵ_V as a function of d and Λ. (For interpretation of the references to color in this figure legend, the reader is referred to the web version of this article.)

4.3. Further constraints from dark photon bounds

Many experimental searches have placed constraints on a massive vector particle V whose field strength mixes with that of hypercharge. These are generally referred to as "dark photon" searches and rely on a combination of precision measurements, searches for rare meson decays, and low-energy collider or fixed target experiments [77,79–81]. Further constraints on the small-mixing regime arise from the effect of dark photon production on energy loss in supernovas [82]. Recent reviews of the status may be found in [83,84]. The continuum that we are interested in is a limiting case of a tower of dark photons with different masses and with a mass-dependent kinetic mixing parameter. Some constraints on dark photons carry over directly to our scenario. Others involve searches for narrow spectral features and no longer apply to a continuum of new particles. However, in the presence of a mass gap, it is quite plausible that near threshold there is a well-defined, narrow single-particle state. In the case that the spectral function consists of a sum over narrow poles from a warped extra dimension, it has been argued that the lightest state will give rise to the most important constraint [39].

One of the strongest constraints for resonances in the mass range of interest, near 10 MeV, is from the NA48/2 experiment at CERN, which searched for decays $\pi^0 \to \gamma V$ with $V \to e^+e^-$ [85]. They have expressed the constraint as an upper bound on ϵ_V^2 which fluctuates, over the mass range 10 MeV $\lesssim m_V \lesssim$ 20 MeV, between about 2×10^{-7} and 8×10^{-7}. Other interesting bounds come from beam dump experiments [81,86,87]. For $\epsilon_V \sim 10^{-3}$, the Fermilab E774 experiment [88] excludes $m_V \lesssim 10$ MeV. For masses 10 MeV $\lesssim m_V \lesssim$ 20 MeV, a combination of the SLAC E141 [89], SLAC E137 [90], KEK [91], and Orsay [92] beam dump experiments exclude a wide range of mixings between about 10^{-8} and few $\times$ 10^{-4}. Supernova constraints further exclude the range $10^{-10} \lesssim \epsilon_V \lesssim 10^{-8}$ for dark photon masses up to around 100 MeV [82,93,94] and the lack of observations related to electromagnetic decays of the dark photon outside the supernova exclude a further range $10^{-12} \lesssim \epsilon_V \lesssim 10^{-10}$ for $m_V \lesssim 20$ MeV [95].

Reanalyzing all available data for the case of a continuum of states is both beyond the scope of this paper and highly model-dependent. Unlike direct detection phenomenology, searches for dark photons directly probe the timelike region of the two-point function for $\mathcal{O}_{\mu\nu}$ and the result can be very sensitive to the detailed mechanism for generating a mass gap. Theories with a sequence of many narrow resonances are subject to a wider variety of direct constraints than theories with a broad continuum. We expect that there will likely be a resonance-like state near the mass threshold, based on analogy to QCD-like theories, but even this is not obviously guaranteed by general principles of quantum field theory. Furthermore, the amount of spectral weight in such a state is not guaranteed; that is to say, we might find that the parameter ξ_V in (31) is significantly smaller than one, relaxing the bounds. Caveats aside, there is essentially only one window in which we might aim for the light state V to lie:

$$2 \times 10^{-4} \lesssim \epsilon_V \lesssim 10^{-3}. \tag{40}$$

with 10 MeV $\lesssim m_V \lesssim$ 20 MeV (to avoid the E774 constraint while still maintaining continuum-like direct detection phenomenology). This window squeezes in between beam dump constraints and the π^0 decay search. The combination of beam dump and supernova constraints rule out all smaller mixings above the BBN constraint (35) and are fairly robust: for instance, even if further dark sector states exist and a decay like $V \to SS$ is allowed and prompt, the S particle will not promptly decay to Standard Model particles unless couplings through portals other than just hypercharge are added to the theory. In the window (40) of allowed ϵ_V, decays of the V particle are prompt on collider length scales and even the BBN constraint (39) for the case of scalar decays is safe.

This constraints are visualized in Fig. 4. We see that for reasonable values of the suppression scale Λ, in the region of allowed ϵ (in blue) the parameter space $d \to 2$ is compatible with suppression scales a few orders of magnitude above the weak scale.

4.4. Constraint from exotic Z decays

Mixing of the Z boson with the operator $\mathcal{O}_{\mu\nu}$ allows the Z to decay into light mediators. These may shower or cascade in various ways, possibly producing a large multiplicity of light particles, like the vector V or scalar S discussed above. Depending on the lifetime of these particles the event could be invisible or there could be distinctive signals involving lepton jets [96], photon jets [97], displaced vertices, or combinations thereof. Without a detailed model, it is difficult to say precisely what the LEP constraint on such exotic decays might be, or even whether the tightest constraint arises from LEP rather than from a hadron collider. Consequently, we will focus on a very robust limit arising from the total width of the Z boson. The Z boson width is measured to be $\Gamma_Z = 2.4952 \pm 0.0023$ GeV [98] whereas the global electroweak fit not including direct measurements of the width gives $\Gamma_Z = 2.4946 \pm 0.0016$ GeV [99]. From these numbers we estimate the constraint on the *total* new physics contribution to the Z boson width,

$$\Gamma_Z^{\text{new}} \lesssim 6 \text{ MeV}. \tag{41}$$

The bound for invisible decays is somewhat stricter, but not dramatically so [100].

We will denote the decay width induced by the mixing of the Z with $\mathcal{O}_{\mu\nu}$ by $\Gamma(Z \to \text{CFT})$, even though a small mass gap may mean that strictly speaking we are not decaying to a conformal sector. To compute this width we exploit the optical theorem, which tells us that $\Gamma(Z \to \text{CFT}) = \frac{1}{m_Z}\text{Im}\mathcal{M}(Z \to Z)$, where $\mathcal{M}(Z \to Z)$ is the amplitude for the Z boson to mix with the mediator and then mix back. The imaginary part of the amplitude comes from the discontinuity across the branch cut in the factor $(-k^2)^{d-2}$ in the two-point function of $\mathcal{O}_{\mu\nu}$: $\text{Disc}\left[(-k^2)^{d-2}\right] = 2i\sin(\pi d)(-k^2)^{d-2}$. Using the identity $\sin(\pi d) = \frac{\pi}{\Gamma(d)\Gamma(1-d)}$, we find

$$\Gamma(Z \to \text{CFT}) = \frac{2\pi c_B^2 \sin^2\theta_W (d-1)(d-2)}{\Gamma(d)\Gamma(d+1)}\left(\frac{m_Z}{2\Lambda}\right)^{2d-4} m_Z. \tag{42}$$

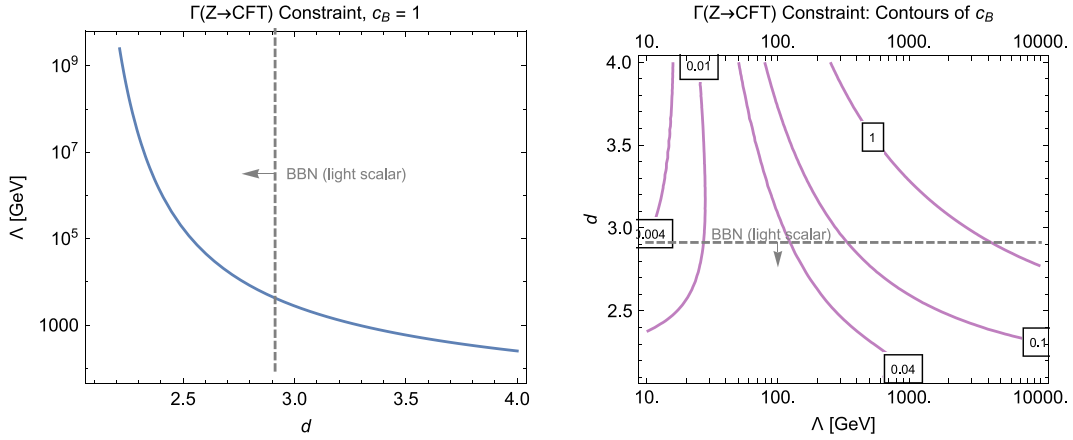

Fig. 5. Constraints on couplings in the theory from the Z boson exotic width. At left, we also fix $c_B = 1$ and plot the largest allowed value of Λ as a function of the operator dimension d. In the region to the left of the dashed line, this value of Λ obeys the constraint (38) for BBN with a 10 MeV scalar as the lightest state; the entire plot obeys the constraint (34) for BBN with a 10 MeV vector lightest particle. At right, we vary Λ and d and plot contours of the largest allowed value of c_B. Again, the dashed line demarcates the part of the plot that is safe from BBN even with a light scalar.

Notice that this decay width goes to zero when $d \to 2$; in this limit the mixing is with a free particle, and the spectral function has no overlap with the Z mass. Comparing Eqs. (41) and (42) gives us a bound on the largest allowed mixing for any model. We plot this bound in Fig. 5. The figure shows that at small values of d, approaching the limit of simple kinetic mixing, the bounds become strong and force us to consider large values of Λ. At larger operator dimensions, the bound is weaker and even relatively low values of Λ are allowed by the data. These large operator dimensions ($d \gtrsim 2.9$) can be in conflict with the BBN constraint (38) in the case that the lightest particle in the mediator sector is a scalar. However, as noted earlier this bound can be avoided by adding more direct couplings of the scalar operator to the SM (e.g. to the Higgs portal) or by unconventional thermal histories of the early universe.

4.5. Maximum total cross sections

The constraints from dark photon searches and new contributions to the Z boson width lead to a maximum possible direct detection cross section for a given operator dimension and value of c_2. We would like to assess how large a total cross section it is reasonable to obtain. However, the total cross section itself is not an ideal quantity to plot. The reason is that, particularly for models that produce distributions dR/dE_R that are highly peaked at low energy transfers, the total cross section may not be reflective of the event rate in a real experiment with a finite energy threshold. (Indeed, the total cross section may not even be defined, for sufficiently singular behavior at low E_R.) As a result, we will define a notion of "effective total cross section".

The typical exclusion plot of an experiment like LUX gives a constraint on the dark matter–proton scattering cross section. Of course, this involves an assumption, and makes the most sense for the case in which the operator involved in the non-relativistic theory is simply 1, e.g. when the underlying relativistic interaction is $\bar{\chi}\chi\bar{N}N$. Thus, to get a rough notion of the total event rate allowed, we take the following definition: For a given model of interest, the **effective dark matter–proton cross section** σ_p^{eff} is defined as the value of σ_p obtained in a model with a 100 GeV Dirac dark matter particle χ scattering through the interaction $\bar{\chi}\chi\bar{p}p$ that gives the *same* integrated rate for scattering on ^{131}Xe over the recoil energy range 3–25 keV as the model of interest. This definition has the disadvantage of making explicit reference to a particular experiment and its range of accessible recoil energies. However, *any* definition of cross section that we compare across different experiments and different models must build in some assumptions. Rigorously speaking, we should fit each individual model across all experiments. For the simple purpose of getting an order-of-magnitude sense of how the scattering rate allowed by our model compares to the scattering rate of a more standard model, on the other hand, σ_p^{eff} is fairly useful.

With these interpretational caveats out of the way, we present the result for the largest σ_p^{eff} allowed by the dark photon and Z width constraints. We compute dR/dE_R for the comparison model, $\mathcal{L} = \frac{f_p}{\Lambda^2}\bar{\chi}\chi\bar{p}p$, using the code of Ref. [4], then numerically integrate over E_R from 3 to 25 keV. For this model, $\sigma_p = \frac{\mu_p^2}{\pi}\left(\frac{f_p}{\Lambda^2}\right)^2$. We also compute dR/dE_R for our model of interest with the same code, putting in a contact interaction and then weighting the answer by appropriate powers of $-q^2$ or of $(-q^2 + m_{\text{gap}}^2)$ to model the continuum exchange. Finally, we scale f_p so that the integrated rates match and read off the corresponding value of σ_p.

The result of this exercise, for dark matter scattering on ^{131}Xe, is presented in Fig. 6. The plot illustrates that there is no allowed cross section when $d \gtrsim 2.6$, because the Z width, beam dump, and supernova constraints forbid all possible $\epsilon_V \gtrsim 10^{-10}$ and smaller ϵ_V are excluded by BBN. For smaller values of d compatible with the range $2 \times 10^{-4} \lesssim \epsilon_V \lesssim 10^{-3}$, the largest allowed cross section is determined mostly by the dark photon constraint when $d \lesssim 2.4$ and mostly by the Z width constraint when $d \gtrsim 2.4$. Notice that the cross sections allowed for EDMs are several orders of magnitude larger than for MDMs. This is because, at fixed coefficient c_B, the non-relativistic scattering through the MDM operator is suppressed by $v^2 \sim 10^{-6}$ relative to that through the EDM operator.

To summarize our results, despite the existence of a variety of stringent constraints on the operator $\mathcal{O}_{\mu\nu}$ coupling to hypercharge, arising from both low-energy probes like beam-dump experiments and pion decay and high-energy probes like Z boson decays, there is a range of dimensions – roughly $2 \lesssim d \lesssim 2.6$ – for which sizable direct detection cross sections could occur. Of course, direct detection experiments themselves can constrain this region. However, due to the unusual spectral shapes that appear in continuum-mediated scattering, a new analysis of the direct detection data will be necessary to derive precise bounds. We leave such analyses for future work.

5. Conclusions

As the simplest models of WIMPs come under strain from a variety of experiments (direct detection, indirect detection,

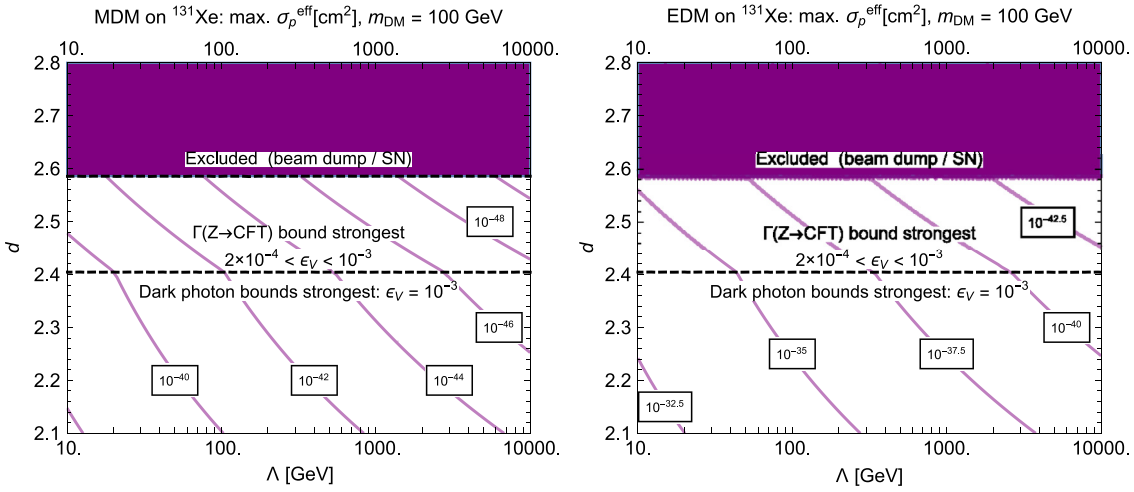

Fig. 6. The largest effective cross section $\sigma_p^{\rm eff}$ for dark matter scattering on ^{131}Xe allowed by the constraints from dark photon searches and the Z boson width. The left-hand plot is for magnetic dipole-type couplings of DM to $\mathcal{O}_{\mu\nu}$ and the right-hand plot for electric dipole-type coupling. We fix $c_2 = 1$ and a dark matter mass of 100 GeV. For a given Λ and d, the largest allowed value of c_B is chosen. At small d this is determined by the dark photon constraint $\epsilon_V \lesssim 10^{-3}$. At somewhat larger $d \gtrsim 2.4$ the Z width becomes the dominant constraint. At the point that the Z width no longer allows $\epsilon_V \gtrsim 2 \times 10^{-4}$, the beam dump and supernova constraints on dark photons force us all the way down to ϵ_V so small that the dark photons would decay after BBN, so no cross section is allowed above $d \approx 2.6$. What is plotted is the cross section σ_p in square centimeters associated to a model with scalar contact interaction achieving the same integrated rate.

and colliders), it becomes increasingly important to broaden our theoretical vision of what dark matter might be. In recent years, a large number of directions have been explored. One common theme is the possibility of a dark sector, with additional new particles beyond the dark matter alone. In this paper we have explored a novel type of dark sector in which the scattering of dark matter with ordinary matter proceeds not through a contact interaction or the exchange of a single particle but through a continuum of mediators.

The basic formalism for direct detection is simple: the continuum mediator multiplies the amplitude by a function of q^2, which in the simplest scale-invariant scenario is just a power law. However, as we have seen, various complications arise. If we wish to have a mass gap to avoid BBN constraints, the direct detection phenomenology can be surprisingly robust, but the constraints imposed on the scenario from other experiments may be very sensitive to the nature of the mass gap. We have explored this in some detail for the case of an antisymmetric tensor mediator coupling to the field strength of hypercharge. A combination of low-energy and high-energy accelerator experiments puts significant restrictions on the allowed parameter space. Nonetheless, we have argued that these constraints still allow room for quite large and detectable signals at direct detection experiments like LUX.

Many aspects of our analysis could be refined in the future, as the interplay between direct detection experiments and other experiments is complex. We have not discussed indirect detection, where the Sommerfeld effect may be relevant (see [37] for related work). The annihilations are expected to proceed dominantly into the states of the approximately conformal sector, undergo complicated cascades and then finally decays into the SM particles. Eventually the annihilation mode closely resembles the hidden valley scenario ($2 \to$ many). This distinctive annihilation pattern together with potential signal in low-energy searches for the light dark photon can potentially help to differentiate this scenario from an ordinary form-factor DM, which otherwise looks identical to the continuum mediated DM scenario in the direct detection experiments. These directions would be interesting to explore further.

Despite these complexities, the picture for direct detection is extremely simple, and searches for unusual dependence of signals on recoil energy are well worth pursuing. It is an exciting possibility that the discovery of dark matter could also be the discovery of a rich, interacting sector that could exhibit novel quantum field theoretic phenomena like scale-invariance in ways that we have not previously seen in particle physics.

Acknowledgments

We thank an anonymous referee for pointing out the importance of supernova constraints on dark photons. The research of AK was partially supported by the Munich Institute for Astro- and Particle Physics (MIAPP) of the DFG cluster of excellence "Origin and Structure of the Universe". MR is supported in part by the NSF Grant PHY-1415548. AK's and MR's work was supported in part by the National Science Foundation under Grant No. PHYS-1066293 and the hospitality of the Aspen Center for Physics. MR would also like to thank the organizers of the 21st International Summer Institute on Phenomenology of Elementary Particles and Cosmology (SI2015) near Beijing for providing a hospitable environment while some of this work was completed.

Appendix. Factorization example: antisymmetric tensor

Let us consider two different scenarios that involve the dark matter tensor current operator $\chi^\dagger \sigma^{\mu\nu} \chi$ coupling to some mediator. The first case is the standard electric or magnetic dipole moment coupling to the photon:

$$\mathcal{L}_1 = c\chi^c \sigma^{\mu\nu} \chi F_{\mu\nu} + \text{h.c.} \tag{43}$$

In the second case, we couple to some more general operator $\mathcal{O}_{\mu\nu}$ of dimension $d \geq 2$ that mixes with the photon's field strength:

$$\mathcal{L}_2 = c_1 \chi^c \sigma^{\mu\nu} \chi \mathcal{O}_{\mu\nu} + \text{h.c.} + c_2 \mathcal{O}_{\mu\nu} F^{\mu\nu}. \tag{44}$$

The question is whether these two Lagrangians can lead to different tensor structures or form factors. We will see that they do not.

In this computation we will use the following two propagators for the photon and the tensor field $\mathcal{O}_{\mu\nu}$:

$$\left\langle A_\mu(q) A_\nu(-q) \right\rangle \equiv \Pi_{\mu\nu}(q) = \frac{1}{q^2}\left(g_{\mu\nu} - \frac{q_\mu q_\nu}{q^2}\right), \tag{45}$$

$$\left\langle \mathcal{O}_{\mu\nu}(q) \mathcal{O}_{\lambda\sigma}(-q) \right\rangle \equiv P_{\mu\nu,\lambda\sigma}(q) \propto -(-q^2)^{d-2} \times \left[\left(g_{\mu\lambda} g_{\nu\sigma} - 2g_{\mu\lambda}\frac{q_\nu q_\sigma}{q^2} - 2g_{\nu\sigma}\frac{q_\mu q_\lambda}{q^2}\right) - (\mu \leftrightarrow \nu)\right]. \tag{46}$$

A.1. Hypercharge with dipole moments

Let us first consider the case of $\mathcal{L}_1$:

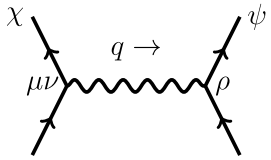

$$\propto J^{\text{dark}}_{\mu\nu}\left(q^{\mu}\Pi^{\nu\rho}(q) - q^{\nu}\Pi^{\mu\rho}(q)\right)J^{\text{SM}}_{\rho}. \tag{47}$$

Because the electromagnetic field strength is dotted into the dark matter tensor current, we have one term where the photon propagator is $\Pi_{\nu\rho}$ and one where it is $\Pi_{\mu\rho}$, each multiplying the appropriate momentum from the derivative from $F_{\mu\nu}$. A little simplification reveals that this amplitude dots the dark tensor current and visible electromagnetic current into the object

$$\mathcal{I}_{\mu\nu,\rho}(q) \equiv q_{\mu}\Pi_{\nu\rho}(q) - q_{\nu}\Pi_{\mu\rho}(q) = \frac{q_{\mu}g_{\nu\rho} - q_{\nu}g_{\mu\rho}}{q^2}. \tag{48}$$

A.2. Antisymmetric tensor mediator

Now we consider the case of $\mathcal{L}_2$, where the coupling is to an antisymmetric tensor field that kinetically mixes with hypercharge:

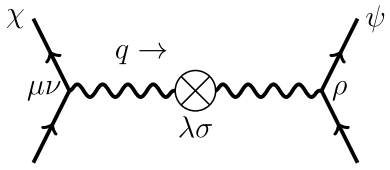

$$\propto J^{\text{dark}}_{\mu\nu}\,P^{\mu\nu,\lambda\sigma}(q)\left(q_{\lambda}\Pi_{\sigma\rho}(q) - q_{\sigma}\Pi_{\lambda\rho}(q)\right)J^{\text{SM}\,\rho}. \tag{49}$$

In this case, we first have the propagator of $\mathcal{O}_{\mu\nu}$ itself, then an insertion which mixes it into electromagnetism, which propagates and couples to the Standard Model current.

In this case, the structure appearing in the middle is

$$\mathcal{I}'_{\mu\nu,\rho}(q) \equiv P_{\mu\nu,\lambda\sigma}(q)\left(q^{\lambda}\Pi^{\sigma}_{\rho}(q) - q^{\sigma}\Pi^{\lambda}_{\rho}(q)\right). \tag{50}$$

Contracting all of the indices and simplifying, we find that

$$\mathcal{I}'_{\mu\nu,\rho}(q) = 2\left(-q^2\right)^{d-2}\mathcal{I}_{\mu\nu,\rho}(q). \tag{51}$$

This shows that the general case of antisymmetric tensor mediator exchange is equivalent to the case of dark matter with dipole moments, reweighted by constant factors times an appropriate power of $-q^2$ where q is the momentum exchanged between dark matter and the Standard Model in the scattering process.

In particular, when the unitarity bound is saturated and $d = 2$, the operator $\mathcal{O}_{\mu\nu}$ is the field strength of an abelian gauge field and this reduces to the usual case of kinetic mixing. In that case, the q dependence is exactly as for ordinary dipole moment dark matter.

A.3. Comment

In fact, this result should follow on general grounds. The amplitude necessarily has the form $J^{\text{dark}}_{\mu\nu}I^{\mu\nu\rho}(q)J^{\text{SM}}_{\rho}$ where $I^{\mu\nu\rho}(q)$ is antisymmetric in μ and ν. The only possible tensor structure is $\mathcal{I}_{\mu\nu,\rho}(q)$. More generally, exchange of a mediator field will always produce at most a small finite set of tensor structures coupling a dark current to a Standard Model current. If an analysis of the full set of tensor structures has been carried out for the exchange of ordinary weakly-coupled particles, then the more general exchange of operators of arbitrary dimension will not lead to new tensor structures or form factors, but only to new momentum dependence in the amplitude.

References

[1] J. Fan, M. Reece, L.-T. Wang, Non-relativistic effective theory of dark matter direct detection, J. Cosmol. Astropart. Phys. 1011 (2010) 042. arXiv:1008.1591 [hep-ph].

[2] A.L. Fitzpatrick, W. Haxton, E. Katz, N. Lubbers, Y. Xu, The effective field theory of dark matter direct detection, J. Cosmol. Astropart. Phys. 1302 (2013) 004. arXiv:1203.3542 [hep-ph].

[3] A.L. Fitzpatrick, W. Haxton, E. Katz, N. Lubbers, Y. Xu, Model independent direct detection analyses, arXiv:1211.2818 [hep-ph].

[4] N. Anand, A.L. Fitzpatrick, W.C. Haxton, Weakly interacting massive particle-nucleus elastic scattering response, Phys. Rev. C 89 (6) (2014) 065501. arXiv:1308.6288 [hep-ph].

[5] A.H.G. Peter, V. Gluscevic, A.M. Green, B.J. Kavanagh, S.K. Lee, WIMP physics with ensembles of direct-detection experiments, Phys. Dark Univ. 5–6 (2014) 45–74. arXiv:1310.7039 [astro-ph.CO].

[6] M.I. Gresham, K.M. Zurek, Effect of nuclear response functions in dark matter direct detection, Phys. Rev. D 89 (12) (2014) 123521. arXiv:1401.3739 [hep-ph].

[7] V. Gluscevic, A.H.G. Peter, Understanding WIMP-baryon interactions with direct detection: A Roadmap, J. Cosmol. Astropart. Phys. 1409 (09) (2014) 040. arXiv:1406.7008 [astro-ph.CO].

[8] R. Catena, Prospects for direct detection of dark matter in an effective theory approach, J. Cosmol. Astropart. Phys. 1407 (2014) 055. arXiv:1406.0524 [hep-ph].

[9] SuperCDMS Collaboration, K. Schneck, et al., Dark matter effective field theory scattering in direct detection experiments, Phys. Rev. D 91 (9) (2015) 092004. arXiv:1503.03379 [astro-ph.CO].

[10] R. Catena, P. Gondolo, Global limits and interference patterns in dark matter direct detection, J. Cosmol. Astropart. Phys. 1508 (08) (2015) 022. arXiv:1504.06554 [hep-ph].

[11] R. Catena, Dark matter directional detection in non-relativistic effective theories, J. Cosmol. Astropart. Phys. 1507 (07) (2015) 026. arXiv:1505.06441 [hep-ph].

[12] B.J. Kavanagh, New directional signatures from the nonrelativistic effective field theory of dark matter, Phys. Rev. D 92 (2) (2015) 023513. arXiv:1505.07406 [hep-ph].

[13] V. Gluscevic, M.I. Gresham, S.D. McDermott, A.H.G. Peter, K.M. Zurek, Identifying the theory of dark matter with direct detection, arXiv:1506.04454 [hep-ph].

[14] B.A. Dobrescu, I. Mocioiu, Spin-dependent macroscopic forces from new particle exchange, J. High Energy Phys. 11 (2006) 005. arXiv:hep-ph/0605342 [hep-ph].

[15] D. Tucker-Smith, N. Weiner, Inelastic dark matter, Phys. Rev. D 64 (2001) 043502. arXiv:hep-ph/0101138 [hep-ph].

[16] P.W. Graham, R. Harnik, S. Rajendran, P. Saraswat, Exothermic dark matter, Phys. Rev. D 82 (2010) 063512. arXiv:1004.0937 [hep-ph].

[17] G. Barello, S. Chang, C.A. Newby, A model independent approach to inelastic dark matter scattering, Phys. Rev. D 90 (9) (2014) 094027. arXiv:1409.0536 [hep-ph].

[18] B. Feldstein, A.L. Fitzpatrick, E. Katz, Form factor dark matter, J. Cosmol. Astropart. Phys. 1001 (2010) 020. arXiv:0908.2991 [hep-ph].

[19] S. Chang, A. Pierce, N. Weiner, Momentum dependent dark matter scattering, J. Cosmol. Astropart. Phys. 1001 (2010) 006. arXiv:0908.3192 [hep-ph].

[20] D. Curtin, Z. Surujon, Y. Tsai, Direct detection with dark mediators, Phys. Lett. B 738 (2014) 477–482. arXiv:1312.2618 [hep-ph].

[21] D. Curtin, Y. Tsai, The double-dark portal, J. High Energy Phys. 11 (2014) 136. arXiv:1405.1034 [hep-ph].

[22] G. Prezeau, A. Kurylov, M. Kamionkowski, P. Vogel, New contribution to wimp-nucleus scattering, Phys. Rev. Lett. 91 (2003) 231301. arXiv:astro-ph/0309115 [astro-ph].

[23] V. Cirigliano, M.L. Graesser, G. Ovanesyan, WIMP–nucleus scattering in chiral effective theory, J. High Energy Phys. 10 (2012) 025. arXiv:1205.2695 [hep-ph].

[24] V. Cirigliano, M.L. Graesser, G. Ovanesyan, I.M. Shoemaker, Shining LUX on isospin-violating dark matter beyond leading order, Phys. Lett. B 739 (2014) 293–301. arXiv:1311.5886 [hep-ph].

[25] J.F. Cherry, M.T. Frandsen, I.M. Shoemaker, Direct detection phenomenology in models where the products of dark matter annihilation interact with nuclei, Phys. Rev. Lett. 114 (2015) 231303. arXiv:1501.03166 [hep-ph].

[26] K. Kumar, A. Menon, T.M.P. Tait, Magnetic Fluffy Dark Matter, J. High Energy Phys. 02 (2012) 131. arXiv:1111.2336 [hep-ph].

[27] K.R. Dienes, B. Thomas, Dynamical dark matter: I. Theoretical overview, Phys. Rev. D 85 (2012) 083523. arXiv:1106.4546 [hep-ph].

[28] K.R. Dienes, B. Thomas, Dynamical dark matter: II. An explicit model, Phys. Rev. D 85 (2012) 083524. arXiv:1107.0721 [hep-ph].

[29] K.R. Dienes, J. Kumar, B. Thomas, Direct detection of dynamical dark matter, Phys. Rev. D 86 (2012) 055016. arXiv:1208.0336 [hep-ph].

[30] J. Fan, A. Katz, L. Randall, M. Reece, Double-disk dark matter, Phys. Dark Univ. 2 (2013) 139–156. arXiv:1303.1521 [astro-ph.CO].

[31] J. Fan, A. Katz, L. Randall, M. Reece, Dark-disk universe, Phys. Rev. Lett. 110 (21) (2013) 211302. arXiv:1303.3271 [hep-ph].

[32] M. McCullough, L. Randall, Exothermic double-disk dark matter, J. Cosmol. Astropart. Phys. 1310 (2013) 058. arXiv:1307.4095 [hep-ph].

[33] J. Fan, A. Katz, J. Shelton, Direct and indirect detection of dissipative dark matter, J. Cosmol. Astropart. Phys. 1406 (2014) 059. arXiv:1312.1336 [hep-ph].
[34] L. Randall, R. Sundrum, An alternative to compactification, Phys. Rev. Lett. 83 (1999) 4690–4693. arXiv:hep-th/9906064 [hep-th].
[35] H. Georgi, Unparticle physics, Phys. Rev. Lett. 98 (2007) 221601. arXiv:hep-ph/0703260 [hep-ph].
[36] B. Grinstein, K. Intriligator, I.Z. Rothstein, Comments on unparticles, Phys. Lett. B 662 (2008) 367–374. arXiv:0801.1140 [hep-ph].
[37] C.-H. Chen, C.S. Kim, Sommerfeld enhancement from unparticle exchange for dark matter annihilation, Phys. Lett. B 687 (2010) 232–235. arXiv:0909.1878 [hep-ph].
[38] E.O. Iltan, The annihilation cross section of dark matter which is driven by scalar unparticle, Acta Phys. Polon. B 44 (8) (2013) 1765–1773. arXiv:1206.6988 [hep-ph].
[39] K.L. McDonald, D.E. Morrissey, Low-energy probes of a warped extra dimension, J. High Energy Phys. 05 (2010) 056. arXiv:1002.3361 [hep-ph].
[40] K.L. McDonald, D.E. Morrissey, Low-energy signals from kinetic mixing with a warped abelian hidden sector, J. High Energy Phys. 02 (2011) 087. arXiv:1010.5999 [hep-ph].
[41] K.L. McDonald, Sommerfeld enhancement from multiple mediators, J. High Energy Phys. 07 (2012) 145. arXiv:1203.6341 [hep-ph].
[42] B. von Harling, K.L. McDonald, Secluded dark matter coupled to a hidden CFT, J. High Energy Phys. 08 (2012) 048. arXiv:1203.6646 [hep-ph].
[43] J. Jaeckel, S. Roy, C.J. Wallace, Hidden photons with Kaluza–Klein towers, arXiv:1408.0019 [hep-ph].
[44] V. Silveira, A. Zee, Scalar phantoms, Phys. Lett. B 161 (1985) 136.
[45] C. Burgess, M. Pospelov, T. ter Veldhuis, The Minimal model of nonbaryonic dark matter: A singlet scalar, Nuclear Phys. B 619 (2001) 709–728. arXiv:hep-ph/0011335 [hep-ph].
[46] B. Patt, F. Wilczek, Higgs-field portal into hidden sectors, arXiv:hep-ph/0605188 [hep-ph].
[47] Y.G. Kim, K.Y. Lee, The Minimal model of fermionic dark matter, Phys. Rev. D 75 (2007) 115012. arXiv:hep-ph/0611069 [hep-ph].
[48] Y.G. Kim, K.Y. Lee, S. Shin, Singlet fermionic dark matter, J. High Energy Phys. 05 (2008) 100. arXiv:0803.2932 [hep-ph].
[49] B. Holdom, Two U(1)'s and epsilon charge shifts, Phys. Lett. B 166 (1986) 196.
[50] B. Batell, M. Pospelov, A. Ritz, Direct detection of multi-component secluded WIMPs, Phys. Rev. D 79 (2009) 115019. arXiv:0903.3396 [hep-ph].
[51] G. Krnjaic, K. Sigurdson, Big bang darkleosynthesis, Phys. Lett. B 751 (2015) 464–468. arXiv:1406.1171 [hep-ph].
[52] E. Hardy, R. Lasenby, J. March-Russell, S.M. West, Big bang synthesis of nuclear dark matter, J. High Energy Phys. 06 (2015) 011. arXiv:1411.3739 [hep-ph].
[53] E. Hardy, R. Lasenby, J. March-Russell, S.M. West, Signatures of large composite dark matter states, J. High Energy Phys. 07 (2015) 133. arXiv:1504.05419 [hep-ph].
[54] S.S. Gubser, AdS/CFT and gravity, Phys. Rev. D 63 (2001) 084017. arXiv:hep-th/9912001 [hep-th].
[55] R.H. Cyburt, B.D. Fields, K.A. Olive, E. Skillman, New BBN limits on physics beyond the standard model from ^{4}He, Astropart. Phys. 23 (2005) 313–323. arXiv:astro-ph/0408033 [astro-ph].
[56] P.A.R. Ade, et al. Planck 2015 results. XIII. Cosmological parameters. arXiv:1502.01589 [astro-ph.CO].
[57] F.-Y. Cyr-Racine, K. Sigurdson, Cosmology of atomic dark matter, Phys. Rev. D 87 (10) (2013) 103515. arXiv:1209.5752 [astro-ph.CO].
[58] F.-Y. Cyr-Racine, R. de Putter, A. Raccanelli, K. Sigurdson, Constraints on large-scale dark acoustic oscillations from cosmology, Phys. Rev. D 89 (6) (2014) 063517. arXiv:1310.3278 [astro-ph.CO].
[59] M.A. Buen-Abad, G. Marques-Tavares, M. Schmaltz, Non-abelian dark matter and dark radiation, Phys. Rev. D 92 (2) (2015) 023531. arXiv:1505.03542 [hep-ph].
[60] J. Lesgourgues, G. Marques-Tavares, M. Schmaltz, Evidence for dark matter interactions in cosmological precision data?, arXiv:1507.04351 [astro-ph.CO].
[61] M. Reece, T. Roxlo, Nonthermal production of dark radiation and dark matter, arXiv:1511.06768 [hep-ph].
[62] CDMS Collaboration, D.S. Akerib, et al., A low-threshold analysis of CDMS shallow-site data, Phys. Rev. D 82 (2010) 122004. arXiv:1010.4290 [astro-ph.CO].
[63] LUX Collaboration, D.S. Akerib, et al., First results from the LUX dark matter experiment at the Sanford Underground Research Facility, Phys. Rev. Lett. 112 (2014) 091303. arXiv:1310.8214 [astro-ph.CO].
[64] A.G. Cohen, H. Georgi, Walking beyond the rainbow, Nuclear Phys. B 314 (1989) 7.
[65] P.J. Fox, A. Rajaraman, Y. Shirman, Bounds on unparticles from the higgs sector, Phys. Rev. D 76 (2007) 075004. arXiv:0705.3092 [hep-ph].
[66] L. Randall, R. Sundrum, A large mass hierarchy from a small extra dimension, Phys. Rev. Lett. 83 (1999) 3370–3373. arXiv:hep-ph/9905221 [hep-ph].
[67] M.J. Strassler, Why unparticle models with mass gaps are examples of hidden valleys, arXiv:0801.0629 [hep-ph].
[68] E.C. Poggio, H.R. Quinn, S. Weinberg, Smearing the quark model, Phys. Rev. D 13 (1976) 1958.
[69] C. Csaki, M. Reece, J. Terning, The AdS/QCD correspondence: Still undelivered, J. High Energy Phys. 05 (2009) 067. arXiv:0811.3001 [hep-ph].
[70] B. Blok, M.A. Shifman, D.-X. Zhang, An Illustrative example of how quark hadron duality might work, Phys. Rev. D 57 (1998) 2691–2700. arXiv:hep-ph/9709333 [hep-ph]. [Erratum: Phys. Rev.D59,019901(1999)].
[71] M.A. Shifman, Quark hadron duality, in: Proceedings, 8th International Symposium on Heavy Flavor Physics (Heavy Flavors 8), p. hf8/013. 2000. arXiv:hep-ph/0009131 [hep-ph]. http://jhep.sissa.it/archive/prhep/preproceeding/hf8/013 [hf8/013(2000)].
[72] M. Pospelov, T. ter Veldhuis, Direct and indirect limits on the electromagnetic form-factors of WIMPs, Phys. Lett. B 480 (2000) 181–186. arXiv:hep-ph/0003010 [hep-ph].
[73] K. Sigurdson, M. Doran, A. Kurylov, R.R. Caldwell, M. Kamionkowski, Dark-matter electric and magnetic dipole moments, Phys. Rev. D 70 (2004) 083501. arXiv:astro-ph/0406355 [astro-ph]. [Erratum: Phys. Rev.D 73, 089903 (2006)].
[74] V. Barger, W.-Y. Keung, D. Marfatia, Electromagnetic properties of dark matter: Dipole moments and charge form factor, Phys. Lett. B 696 (2011) 74–78. arXiv:1007.4345 [hep-ph].
[75] A.L. Fitzpatrick, K.M. Zurek, Dark moments and the DAMA-CoGeNT puzzle, Phys. Rev. D 82 (2010) 075004. arXiv:1007.5325 [hep-ph].
[76] T. Banks, J.-F. Fortin, S. Thomas, Direct detection of dark matter electromagnetic dipole moments, arXiv:1007.5515 [hep-ph].
[77] M. Pospelov, Secluded U(1) below the weak scale, Phys. Rev. D 80 (2009) 095002. arXiv:0811.1030 [hep-ph].
[78] A. Fradette, M. Pospelov, J. Pradler, A. Ritz, Cosmological constraints on very dark photons, Phys. Rev. D 90 (3) (2014) 035022. arXiv:1407.0993 [hep-ph].
[79] B. Batell, M. Pospelov, A. Ritz, Probing a secluded U(1) at B-factories, Phys. Rev. D 79 (2009) 115008. arXiv:0903.0363 [hep-ph].
[80] M. Reece, L.-T. Wang, Searching for the light dark gauge boson in GeV-scale experiments, J. High Energy Phys. 07 (2009) 051. arXiv:0904.1743 [hep-ph].
[81] J.D. Bjorken, R. Essig, P. Schuster, N. Toro, New fixed-target experiments to search for dark gauge forces, Phys. Rev. D 80 (2009) 075018. arXiv:0906.0580 [hep-ph].
[82] E.W. Kolb, R.N. Mohapatra, V.L. Teplitz, New supernova constraints on sterile neutrino production, Phys. Rev. Lett. 77 (1996) 3066–3069. arXiv:hep-ph/9605350 [hep-ph].
[83] J. Jaeckel, A force beyond the Standard Model—Status of the quest for hidden photons, Frascati Phys. Ser. 56 (2012) 172–192. arXiv:1303.1821 [hep-ph].
[84] R. Essig, et al. Working group report: New light weakly coupled particles, in: Community Summer Study 2013: Snowmass on the Mississippi (CSS2013) Minneapolis, MN, USA, July 29–August 6, 2013. 2013. arXiv:1311.0029 [hep-ph]. http://inspirehep.net/record/1263039/files/arXiv:1311.0029.pdf.
[85] NA48/2 Collaboration, J.R. Batley, et al., Search for the dark photon in π^0 decays, Phys. Lett. B 746 (2015) 178–185. arXiv:1504.00607 [hep-ex].
[86] S. Andreas, C. Niebuhr, A. Ringwald, New limits on hidden photons from past electron beam dumps, Phys. Rev. D 86 (2012) 095019. arXiv:1209.6083 [hep-ph].
[87] J. Blümlein, J. Brunner, New exclusion limits on dark gauge forces from proton bremsstrahlung in beam-dump data, Phys. Lett. B 731 (2014) 320–326. arXiv:1311.3870 [hep-ph].
[88] A. Bross, M. Crisler, S.H. Pordes, J. Volk, S. Errede, J. Wrbanek, A search for shortlived particles produced in an electron beam dump, Phys. Rev. Lett. 67 (1991) 2942–2945.
[89] E.M. Riordan, et al., A search for short lived axions in an electron beam dump experiment, Phys. Rev. Lett. 59 (1987) 755.
[90] J.D. Bjorken, S. Ecklund, W.R. Nelson, A. Abashian, C. Church, B. Lu, L.W. Mo, T.A. Nunamaker, P. Rassmann, Search for neutral metastable penetrating particles produced in the SLAC beam dump, Phys. Rev. D 38 (1988) 3375.
[91] A. Konaka, et al., Search for neutral particles in electron beam dump experiment, Phys. Rev. Lett. 57 (1986) 659.
[92] M. Davier, H. Nguyen Ngoc, An unambiguous search for a light higgs boson, Phys. Lett. B 229 (1989) 150.
[93] J.B. Dent, F. Ferrer, L.M. Krauss, Constraints on light hidden sector gauge bosons from supernova cooling, arXiv:1201.2683 [astro-ph.CO].
[94] H.K. Dreiner, J.-F. Fortin, C. Hanhart, L. Ubaldi, Supernova constraints on MeV dark sectors from e^+e^- annihilations, Phys. Rev. D 89 (10) (2014) 105015. arXiv:1310.3826 [hep-ph].
[95] D. Kazanas, R.N. Mohapatra, S. Nussinov, V.L. Teplitz, Y. Zhang, Supernova bounds on the dark photon using its electromagnetic decay, Nuclear Phys. B 890 (2014) 17–29. arXiv:1410.0221 [hep-ph].
[96] N. Arkani-Hamed, N. Weiner, LHC signals for a superunified theory of dark matter, J. High Energy Phys. 12 (2008) 104. arXiv:0810.0714 [hep-ph].
[97] S.D. Ellis, T.S. Roy, J. Scholtz, Phenomenology of photon-jets, Phys. Rev. D 87 (1) (2013) 014015. arXiv:1210.3657 [hep-ph].
[98] Particle Data Group Collaboration, K.A. Olive, et al., Review of particle physics, Chin. Phys. C 38 (2014) 090001.
[99] Gfitter Group Collaboration, M. Baak, J. Cuth, J. Haller, A. Hoecker, R. Kogler, K. Moenig, M. Schott, J. Stelzer, The global electroweak fit at NNLO and prospects for the LHC and ILC, Eur. Phys. J. C 74 (2014) 3046. arXiv:1407.3792 [hep-ph].
[100] M. Carena, A. de Gouvea, A. Freitas, M. Schmitt, Invisible Z boson decays at e+ e- colliders, Phys. Rev. D 68 (2003) 113007. arXiv:hep-ph/0308053 [hep-ph].